DESIGN AND RESULTS FROM A PROTOTYPE PASSIVE HYDROGEN MASER FREQUENCY STANDARD

F. L. Walls

Frequency & Time Standards Section
National Bureau of Standards
Boulder, Colorado   80302

ABSTRACT

The basic design of a prototype passive hydrogen maser fre-
quency standard is very briefly described and its unique features
outlined. The latest results on its long-term stability and envi-
ronmental sensitivity will be given. The present results indicate
that $\sigma_y(\tau) \le 2 \times 10^{-12} \tau^{-\frac{1}{2}}$ for averaging times between 40 s and
15000 s, $\sigma_y(15000) \sim 1.4 \times 10^{-14}$. Over a fourteen-day period the
rms daily time fluctuations was 2 ns while the least squares fit
to a linear frequency drift over the fourteen days was 6×10^{-16}/day,
which is within the measurement noise. These results are particu-
larly noteworthy for those interested in clocks for timekeeping
applications as they were obtained without temperature control of
any of the electronics and only a single oven on the cavity. Fur-
ther improvements in the electronics including temperature stabili-
zation of critical control circuits should reduce the daily varia-
tions by a factor of five to ten and also improve the already
excellent long-term stability.

The design principles illustrated by this prototype can also
be used to realize a miniature passive hydrogen maser frequency
standard with little compromise in long-term stability [1].

Fig. 1 shows the block diagram of the present prototype passive
hydrogen maser frequency standard. This present configuration is inten-
ded to show feasibility of achieving GPS specifications for time keeping
stability of 10 ns over a 10 day prediction period, and to allow monitor-
ing of various parameters which might affect its performance. The micro-
wave cavity, atomic hydrogen source, and magnetic field configuration are
similar to designs used in active masers. The 5 MHz crystal controlled
oscillator is distributed through five -120 dB isolation amplifiers.
Three outputs are for measurement purposes and two drive internal elec-
tronics. The 5 MHz signal is phase modulated at 12.2 kHz and $\sim$ .4 Hz,
multiplied to 1440 MHz and then mixed with a synthesizer signal to
produce the hydrogen resonance frequency. The .4 Hz phase modulation
probes the hydrogen resonance which produces amplitude modulation at .4
Hz, the size of which is proportional to the frequency offset between

the probe signal and the hydrogen resonance. This signal is detected as .4 Hz amplitude modulation of the 20 MHz signal. After amplification and filtering, this signal is demodulated to produce an error signal which is used to correct the frequency of the 5 MHz oscillator. The attack time of this frequency lock loop is typically a few seconds.

In a very similar way the cavity detuning from the probe frequency is sensed by detecting the 12 kHz amplitude modulation on the 20 MHz signal. This 12 kHz signal is amplified, filtered, and demodulated to produce an error signal which is used to correct the cavity frequency. Since the probe signal is automatically steered to the center of the hydrogen resonance frequency via the .4 Hz servo, this produces a clean way of tuning the cavity frequency to the hydrogen resonance frequency. The 12 kHz sidebands due to the phase modulation are -10 dB relative to the carrier and equal in amplitude to several parts per million. The signal-to-noise in the cavity servo loop is such that the cavity frequency can be detected with a resolution of 5 Hz in only a few seconds. The present servo attack time is 10 s which allows rapid correction of cavity offset due to any environmental perturbation be it changes in pressure, aging of the cavity coating, deformation of the cavity due to strain or sudden shock, or even changes is cavity pulling due to changes of the coupling to the amplifiers. This cavity servo scheme should have virtually no effect on the hydrogen resonance line due to the small size of the 12 kHz sidebands and their high symmetry about the hydrogen resonance.

The ability of the cavity servo to correct for cavity changes is very clearly illustrated by Figure 2. The lower portion shows the cavity correction vs time after a 1°C change in cavity temperature. The sensitivity is about 1 volt per 1 kHz change in uncorrected cavity frequency. The upper portion of Figure 2 shows the frequency of the fully locked up passive hydrogen frequency standard over the same period of time. The frequency changed fractionally by about 7×10^{-14} due to a .7°C change in cavity temperature over the period in which the data was taken. This corresponds to an open loop change of about 700 Hz in cavity frequency. This fractional change of 7×10^{-14} is probably due to a combination of a change in the wall shift and the second order Doppler shift, rather than an error in the cavity servo. Without the cavity servo the frequency would have changed fractionally by $\sim 10^{-11}$. These results mean that the cavity servo can correct for cavity changes of order 100 Hz or larger and still hold the perturbation to the output frequency below 1×10^{-14}. This relaxes the requirement of temperature stability of the cavity approximately a factor of 100 compared to any present stand alone active cavity maser design. The required cavity temperature stability for the passive maser is determined by the second order Doppler shift of 1.3×10^{-13}/°C and the temperature dependence of the wall shift. This limit is about $\pm$ .070°C for a fractional change of $\pm 1 \times 10^{-14}$.

Other parameters which might affect the frequency of such a passive hydrogen maser are variations in hydrogen beam density and variations in microwave power. Fig. 3 shows the data taken to measure the spin-exchange shift. A 33% increase in beam intensity produced a change of $\simeq 6 \pm 4 \times 10^{-14}$. Similarly it was found that a change in microwave power of -2 dB caused a shift of about $8 \pm 4 \times 10^{-14}$. Both these effects are small enough that they should not affect the stability on the 10^{-14} level in the final design. The time domain stability of the passive hydrogen maser for 2000 s < τ < 2.9d was measured against two high-performance cesium tubes in a three-corner hat arrangement, i.e., three pairs of beat frequency data were used to assign a stability to each clock. See Fig. 4.

Figure 4 shows primarily that the frequency stability of the passive hydrogen maser is substantially better than that of Cs 324 and Cs 323, over the region from 2000 s to 64000 s. For example, the data at 2000 s and 4000 s, which have the best confidence, indicate that the short-term stability of the passive hydrogen is $\sim 6 \pm 27 \times 10^{-13} \tau^{-1/2}$. Unfortunately, there just was not enough time to take more data in order to reduce the uncertainty in the measurement.

The data of passive hydrogen versus NBS-6, one of our primary cesium standards is shown in Fig. 5. This data shows that the stability of the pair is $\sim 2.2 \times 10^{-12} \tau^{-1/2}$ (38 s < τ < 15000 s) and hence provides an upper limit on the stability of the passive hydrogen and NBS-6. The long-term frequency stability of the passive hydrogen maser was assessed by comparison against the UTC(NBS) time scale comprised of nine cesium standards including our primary cesium standards NBS-4 and NBS-6. The 5 MHz output from the passive maser was divided down to 1 pulse per second and compared to a similar 1 pulse per second tick originating from member clocks of the time scale. Daily time differences were recorded with an accuracy of $\simeq$ 1.5 ns. In this way the frequency of the passive maser at one-day and longer averaging times could be measured. Frequency stability plots of this data are shown in Figs. 5 and 6. The fractional frequency stability data is shown at the bottom of Fig. 6 along with various notes of prevailing experimental conditions. As noted this data was taken over several days following $\simeq$ 1°C change in cavity temperature. The data over the days 8-9 and 9-10 were anomalously low and an examination of the various monitors indicated that the crystal oscillator servo loop was exceeding its dynamic range part of the time. The crystal oscillator was then re-set within its normal range. The frequency then returned to its nominal average of the first eight days. The morning of day 14, the laboratory suffered a short power outage which caused some troubles in the electronics and the analysis was terminated.

The square root of the Allan Variance derived from the data of Fig.6 is shown in Fig. 5 [2]. It is quite apparent that there is a more or less daily variation in the frequency due to some environmental influence, which is above the level of white frequency fluctuations expected on the basis of the data from 38 s to 15000 s.

In spite of this, the stability at 3 days is $8.4 \pm 5 \times 10^{-15}$ and at 4 days it is $2.2 \pm 1.8 \times 10^{-15}$. It is expected that the noise level near 1 day, which acts like some sort of phase modulation can be reduced by temperature control of the critical servo control electronics and some of the filters. At the present time none of the electronics is temperature controlled. A least squares fit to the data of Fig. 6 yields a linear drift of 6×10^{-16}/day which is within the measurement noise of the two end points. From the frequency stability data of Fig. 6 it can be shown that the expected time keeping accuracy over a 10-day prediction period has a 1σ uncertainty of less than 10 ns. In fact over the 8-day period where continuous data exists, the maximum time excursion was 4 ns using an after the fact average frequency, which of course can't be done for true time prediction.

The <u>long-term</u> frequency stability data presented in Figs. 4 to 6, and especially the low drift are to my knowledge, the best that have ever been documented for a single stand alone hydrogen frequency standard, and it is as good as that observed with multiple hydrogen masers which are autotuned against one another or against a separate hydrogen maser [3-7].

This excellent long-term stability has been accomplished with a relatively standard physics package - only the electronics design is new and it isn't even temperature stabilized yet. Therefore, stabilities of this level or better could be achieved with many existing active masers by converting the electronics to the passive approach outlined in Fig. 1. The main requirement is that the cavity have 2 coupling ports.

The passive electronics will also be used with a small dielectric cavity measuring $\sim 6"$ diameter and 6" long. It is expected that 10-day stabilities exceeding 1×10^{-14} can also be achieved with the small cavity. This coupled with the other advantages of the passive approach, e.g., low hydrogen beam requirements, should make possible a hydrogen maser of exceptional stability measuring less than 15" dia and 36" long.

Moreover it should be reiterated that the sensitivity of the passive hydrogen maser to environmental purturbations is greatly reduced over that of the present stand alone active masers because of its rapid active cavity control, the lack of threshold conditions on beam flux, and its ability via equalization of the populations of the three upper spin states, to greatly reduce the magnetic field inhomogeneity shift (Crampton effect) without reducing the safety margin above a threshold condition [1].

ACKNOWLEDGMENTS

REFERENCES

[1]   F. L. Walls and H. Hellwig, Proc. 30th Annual Frequency
        Control Symp., Ft. Monmouth, NJ (1976).

[2]   J. A. Barnes et al., IEEE Trans. on Instr. and Meas.
        IM-20, No. 2, p. 105 May 1971.

[3]   D. Morris and K. Nakagiri, Metrologia 12, 1, (1976).

[4]   Octav Gheorghiu, Jacques Viennet, Pierre Petit et
        Claude Audoin, C.R. Acad. Sc. Paris t. 278,
        1059, June 1974.

[5]   C. Finnie, R. Sydnor and A. Sward, Proc. 25th Annual
        Freq. Control Symp., Ft. Monmouth, NJ, 348 (1971).

[6]   M. W. Levine, R.F.C. Vessot, E.M. Mattison,
        D.F. Graveline, T.E. Hoffman and R.L. Nicoll, Proc.
        8th Annual Precise Time and Time Interval Applications
        and Planning Meeting, Washington, DC (1976).

[7]   S. Petty, R. Sydnor and P. Dachel, Proc. 8th Annual
        Precise Time and Time Interval Application and
        Planning Meeting, Washington, DC (1976).

FIGURE CAPTIONS

Fig. 1   Block diagram of passive hydrogen maser frequency standard.

Fig. 2   Top: Beat period between NBS-6 and passive hydrogen maser
                during temperature transient of 0.7°C.
          Bottom: Cavity correction during a 0.7°C temperature
                transient.

Fig. 3   Beat period between passive hydrogen maser and NBS-6 at

          5 MHz for hydrogen pressure of 4.11   Pascals (0.309

          Torr) and 5.47   Pascals (0.411 Torr).

Fig. 4   Stability plot for three concurrent beat frequencies between
          Cs 323, Cs 324, and passive hydrogen. This data was then
          used to estimate an independent stability for the passive
          hydrogen maser prototype. The dotted lines are only shown
          to provide a reference. The data spanned 6 days.

Fig. 5   Summary of time domain stability for the present passive
          hydrogen maser. The data vs. NBS-6 (38 s $\leq \tau \leq$ 150 00 s)
          provides an upper limit for the stability of the passive
          hydrogen maser. The passive H estimate is from Fig. 4,
          while the stability of the passive H maser vs. UTC(NBS) was
          calculated from the data shown in Fig. 6. See text.

Fig. 6   Top: Time error of passive hydrogen maser vs. UTC(NBS)
                assuming an average frequency difference of 8900 ns/day
                (rms time error 1.8 ns).
          Bottom: Rate of passive hydrogen vs. UTC(NBS). Note the
                indication of various experimental conditions during
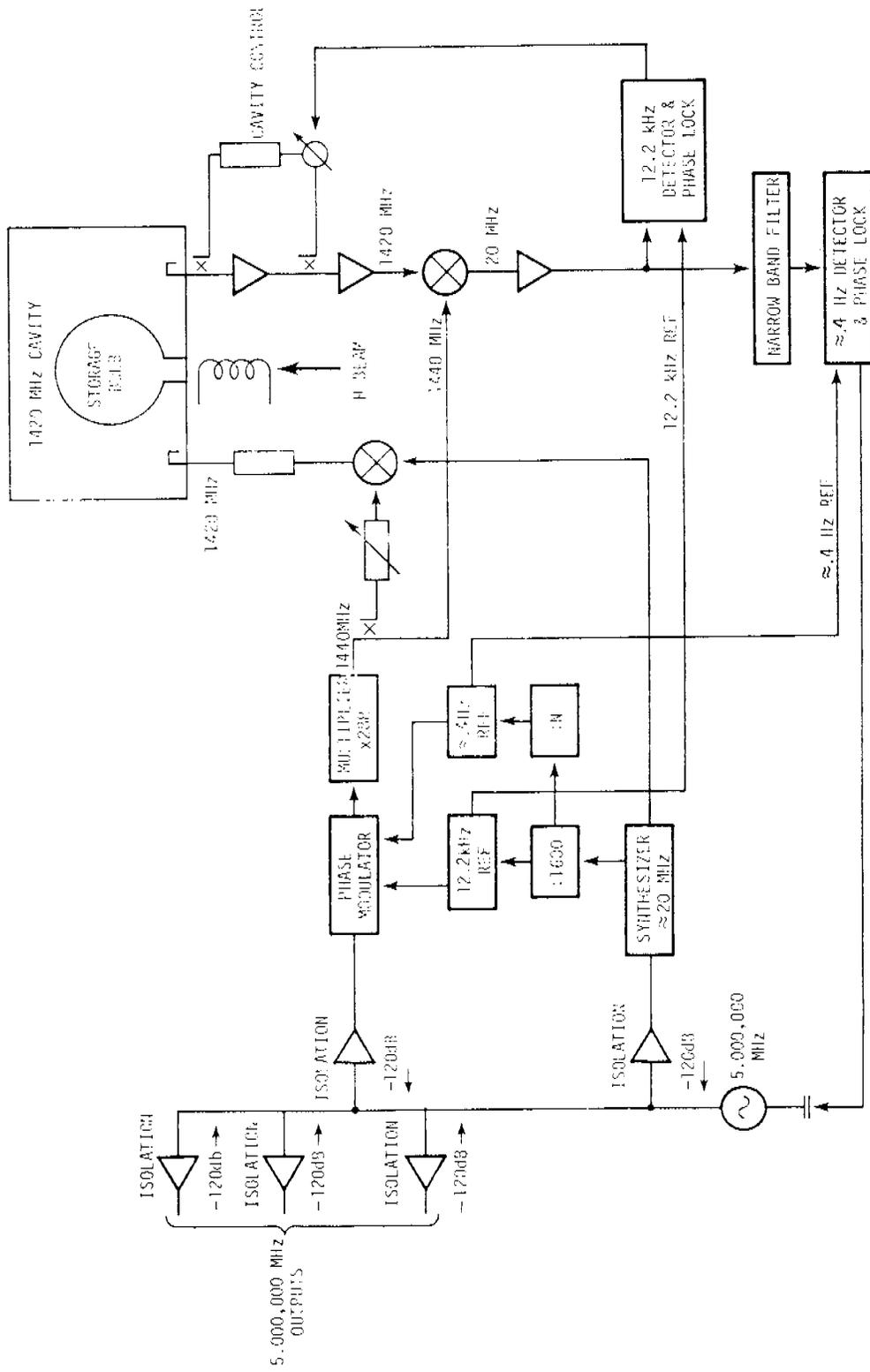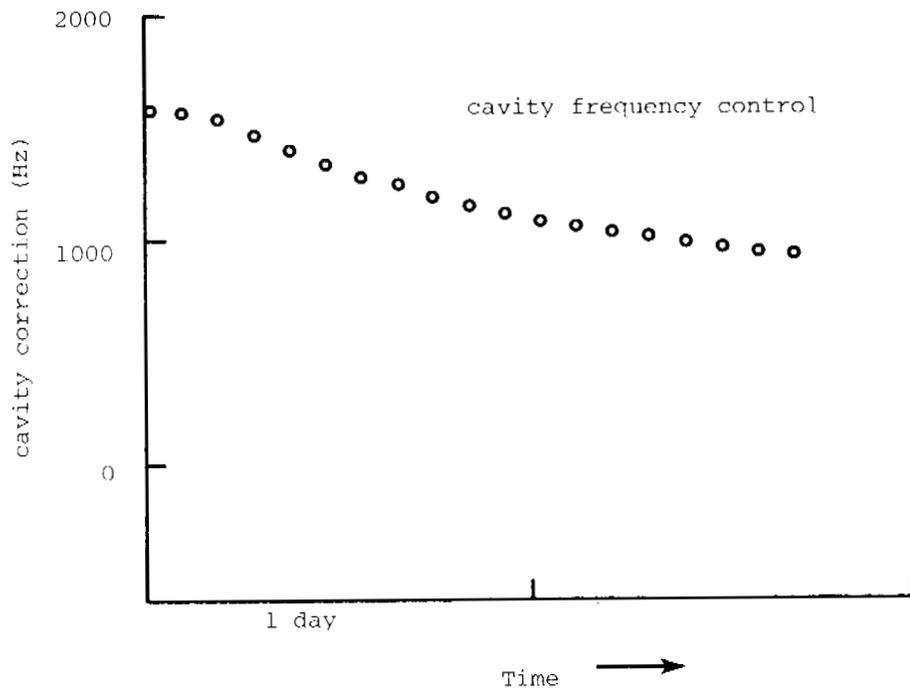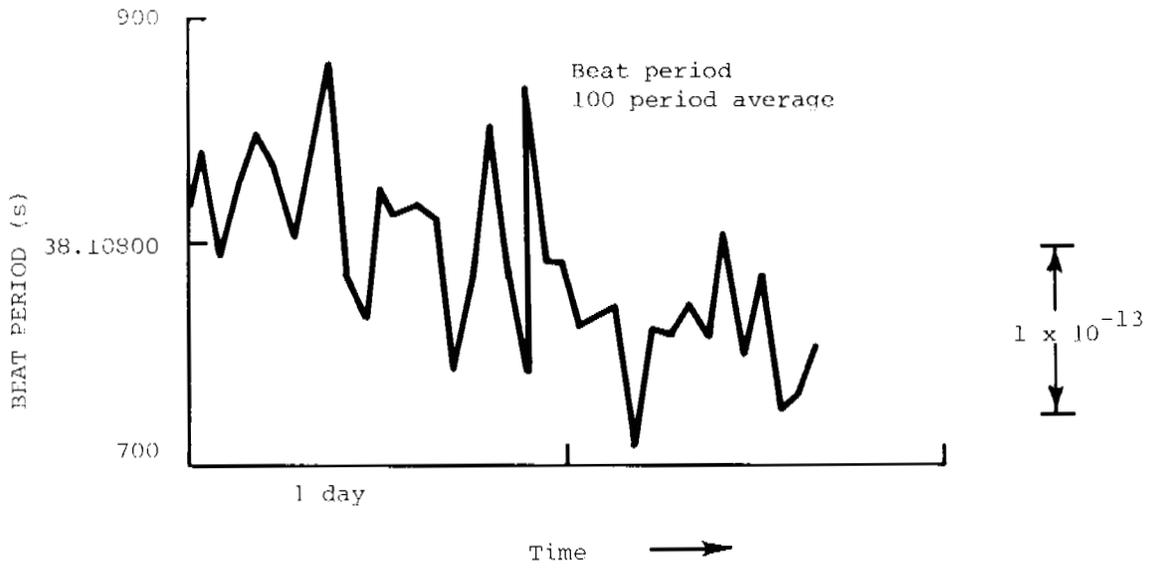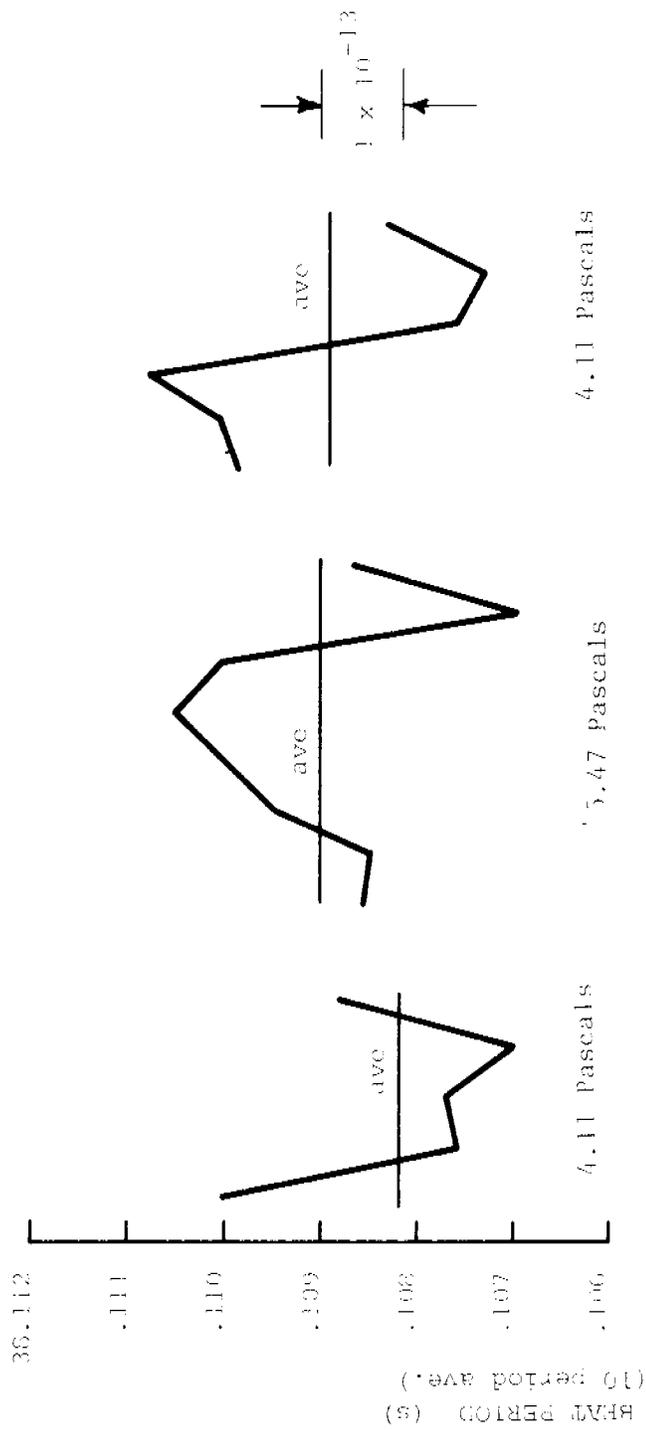   the 14 days.

FIGURE 1

Fig. 2

1×10^{-13}

ave

ave

ave

4.11 Pascals

5.47 Pascals

4.11 Pascals

PRESSURE

FIGURE 3

36.112

.111

.110

.109

.108

.107

.106

BEAT PERIOD (s)
(10 period ave.)

SAMPLE TIME, τ (s)

FIG. 4

378

Fig. 5

379

Fig. 6

8900

10^{-13}

Power outage

5 MHz osc reset

5 MHz osc beyond lock range

$\Delta\nu/\nu = 6 \times 10^{-16}/d$

Time (d)

0 1 2 3 4 5 6 7 8 9 10 11 12 13 14 15

26 Oct.

1°C temp change on 21 Oct.

+4
0
-4

Time Error (ns)

912
908
904
8900
896
892
888

Passive H – UTC(NBS)   (ns/d)

380